Nuclear Mathematical and Computational Sciences: A Century in Review, A Century Anew
Gatlinburg, Tennessee, April 6-11, 2003, on CD-ROM, American Nuclear Society, LaGrange Park, IL (2003)

PRESSURE VESSEL CALCULATIONS FOR VVER-440 REACTORS

E. Temesvári, G.Hordósy,
Gy.Hegyi, A.Keresztúri, Cs.Maráczy, P.Vértes
KFKI Atomic Energy Research Institute
Budapest, Hungary
temese@sunserv.kfki.hu; hordosy@sunserv.kfki.hu

É.Zsolnay
Institute of Nuclear Technique,
Budapest University of Technology and Economics
Budapest, Hungary
zsolnay@reak.bme.hu

ABSTRACT

Monte Carlo calculations were performed for a selected cycle of the Paks NPP Unit II to test a computational model for pressure vessel calculations. In the model the source term was calculated by the core design code KARATE and the neutron transport calculations were performed by the MCNP. The calculated results were compared with measurements and in most cases fairly good agreement was found.

Key Words: pressure vessel, MCNP, cross sections uncertainty, measurements and calculations.

1.INTRODUCTION

Hungary has four units of VVER-440 pressurized water reactor at the Paks Nuclear Power Plant. The lifetime of these units directly depends on the irradiation of the pressure vessel. The flux at the pressure vessel may change essentially with time because of the change in loading strategy and operational conditions. For accurate calculations of the fluence of pressure vessel the change of the neutron source in the core should be considered. At Paks NPP the KARATE code system is to be used to account this change. The particle transport has been studied by the MCNP. As an example, the cycle 8 of the unit II. has been investigated in more detail in this paper.

Some characteristics of the VVER-440 reactors is given in Section 2.1. A short overview of the code system KARATE is presented in Sect. 2.2. The Monte Carlo model is described in 2.3. The calculated and the measured data are presented and discussed in Section 3. The sensitivity of the results for the uncertainties of the iron cross section is also discussed in Section 3. A brief summary is given in Section 4.

2. DESCRIPTION OF THE MODELl

2.1 The VVER-440 Reactors

A VVER-440 core is made up from 349 hexagonal fuel assemblies, each consisting from 126 fuel pins. The lattice pitch of the assemblies is 14.7 cm, the axial height of the active part is 244 cm. In the case investigated in this paper the assemblies had no enrichment zoning. The enrichments are 3.6 %, 2.4 % and 1.6 %. The thermal power of such a unit is 1375 MW. Outside the core the reactor is consisting of the following major components: water, baffle plate (liner), water, core basket, water, core barrel, detector chains, water gap, clad on the pressure vessel, reactor vessel, cavity and the biological shield made up from concrete. In the calculation used in this work a 60-degree sector of the reactor was investigated. On the two sides of the 60-degree region reflective boundary condition was applied. On the outer surface of the concrete black boundary condition was given.

Around the core 6 irradiation places can be found. At each irradiation places there are 2 irradiation capsule assemblies in capsule holder tubes. A typical assembly consists of 19 or 20 capsules. They are located at the azimuthal flux maximum. The capsules contains several kinds of activation foils and Charpy impact test specimens made of reactor vessel material. The detector chains can be found next to the core barrel with a stainless steel cover. The capsule assemblies with the test specimens and activation foils were modeled in detailed in the MCNP calculation.

2.2 The KARATE code system

Our calculations for generating the source for the MCNP Monte Carlo code were made by using the KARATE program system. KARATE is a 3D coupled neutron physical- thermohydraulical core design code developed in KFKI AERI [1] [2]. It solves the neutron transport equation in linearly anisotropic approximation, i.e. the neutron flux and current is calculated. It was validated against a number of measurements and benchmarks. It is routinely used at Paks NPP. It consists of 4 levels of calculations with consistent bi-directional connection between levels via parameterization:

1st level: Multigroup spectral calculations to determine the cross sections for the 2- or 4-group calculations and the energy spectra of the neutron flux and current. 35 thermal and 35 epithermal group is used.

2nd level: 4-group, 2-dimensional fine mesh reflector albedo calculations to evaluate the core-reflector albedo matrices

3rd level: 2-group, two-dimensional fine-mesh calculations, which determine the linear power distribution of the fuel rods. From these calculations the fission source for every level of the fuel rods and for every isotope can be determined

4th level: core-level, nodal calculations, which calculate the power distribution at the assembly level and the boundary conditions for the 3rd level of the calculations.

Using KARATE for pressure vessel source calculations, the reactor core was divided into ten axial layers.

2.3 The MCNP source model

The features of KARATE summarized above offer different possibilities for the definition of the source for Monte Carlo [4] calculations. In the investigations presented in this paper a surface source on the outer surfaces of the outermost fuel assemblies was used. An axial segment of an outer surface of a fuel assembly in the outermost row is called as "page" in the following. By means of KARATE the surface flux and current can be evaluated in 70 energy group for each page, i.e. the angular neutron flux on pages is given in the form

$$\Phi\,(\mathbf{r},E,\mathbf{\Omega}) = 1/4\pi\;\Phi_0\,(\mathbf{r},E) \;+ 3/4\pi\;J(\mathbf{r},E)\;(\mathbf{n\Omega}) \qquad (1)$$

where **n** is the surface normal, Φ_0 is the scalar flux and J is the current. The corresponding surface source can then be written as

$$S_i\,(E,\mathbf{\Omega}) = S_{i,1}\,(E)\;(\mathbf{n\Omega}) + S_{i,2}\,(E)\;(\mathbf{n\Omega})^2 \qquad (2)$$

where the index i refers to a particular page. Using this result, the source can be defined for each page as a weighted sum of a linearly and a quadraticaly anisotropic term. The weights depend on the energy and on the page. MCNP can not handle double-dependence of a variable, but the calculation can be performed in two steps, performing one calculation with linearly and one calculation with quadraticaly anisotropic angular dependence of the source.

3. DESCRIPTION OF THE RESULTS

3.1 Comparison of the calculated and measured results

To test the surface source method by measurements, cycle-averaged reaction rates were calculated for the 8th cycle of Unit II. of Paks NPP for such neutron activation detectors, which were removed from the reactor after one cycle. Load follow calculations were performed for cycles 1-8. During the 8th cycle, the surface source was calculated by KARATE for four values of the effective time to get an accurate representation of the source change. Using these sources, MCNP calculations were performed to evaluate the reaction rates and fast fluxes due the four states of the core, then that the time-integrated values of these quantities were determined. The fast flux is important to investigate the pressure vessel fluence, but for testing the calculational model the reaction rates are used which can be compared with measurements. The fast flux was determined in different positions of the pressure vessel: in the clad of, at the quarter part of (T/4), half part of (T/2) and the outer part of (T) the vessel. The fast reactions Nb93(n,n'), Fe54(n,p) and Cu63(n,α) were examined at surveillance positions and in the cavity at different axial heights. The thermal reactions Nb93(n,γ) and Co59(n,γ) were examined at surveillance position close to the midplane.

The cross sections used in the Monte Carlo calculations were selected from the libraries delivered together with the MCNP by the NEA. For the structural materials ENDF/B-V based cross sections were used. Cross sections made by the Lawrence Livermore National Laboratory

(.30y in MCNP terminology) were used for the reactions of Nb93(n,n') and Fe54(n,p). ENDF/B-VI cross sections were used for the Cu63(n,α), Nb93(n,γ) and Co59(n,γ) reactions.
The comparison of calculated and measured values is shown on the next figures.

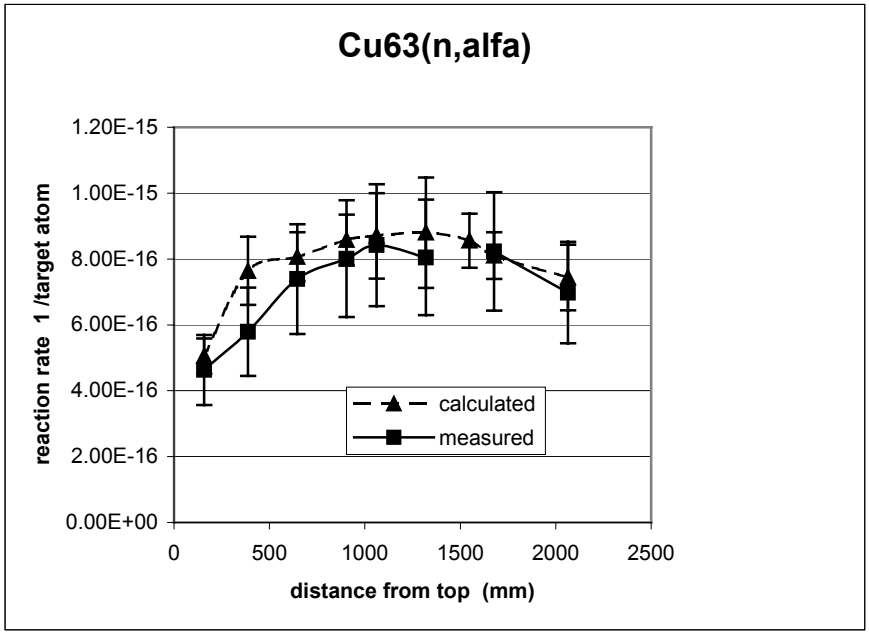

Figure 1. Calculated and measured values of Cu63(n,α) rates at surveillance positions

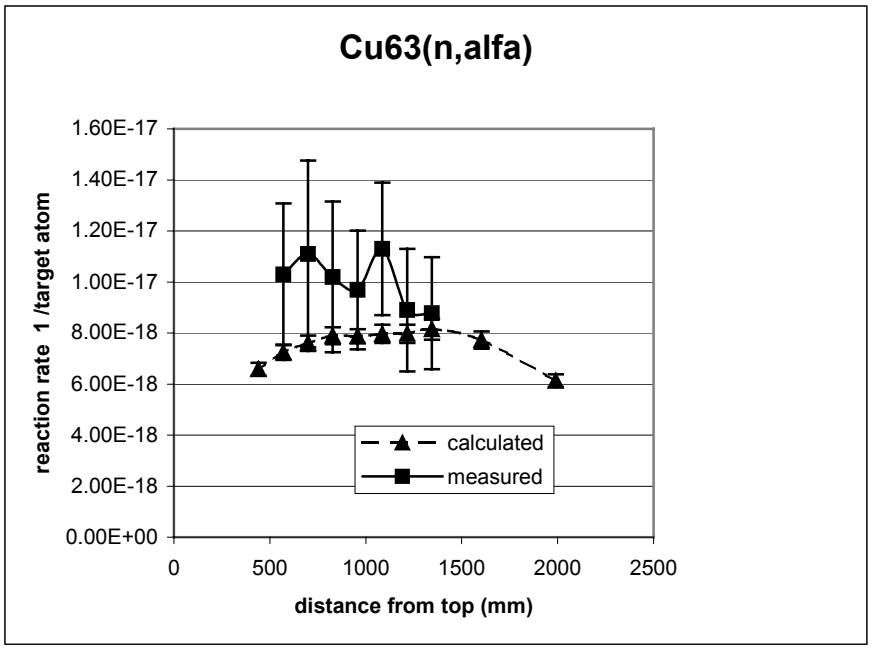

Figure 2. Calculated and measured values of Cu63(n,α) rates in the cavity

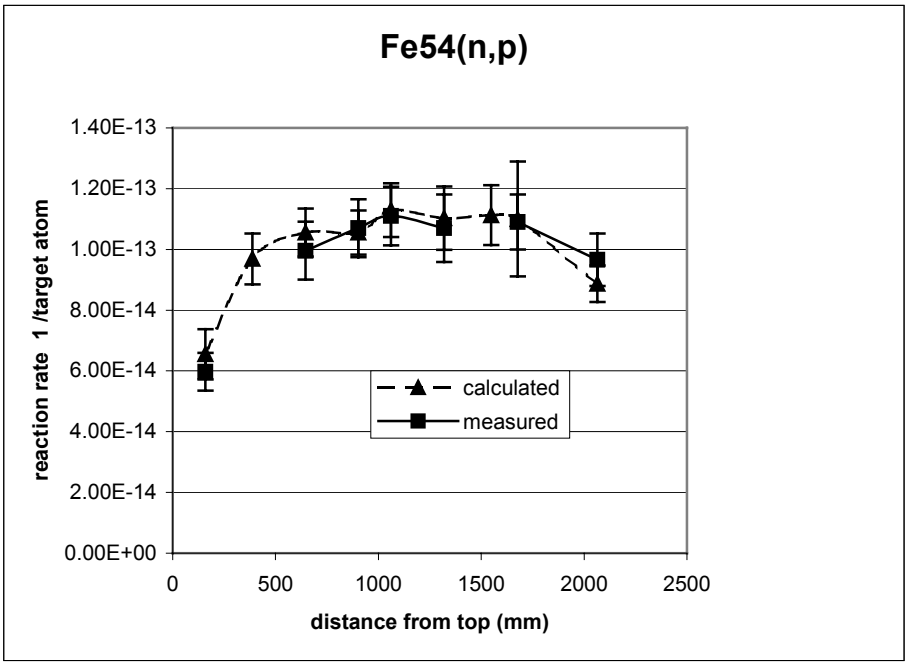

Figure 3. Calculated and measured values of Fe54(n,p) rates at surveillance positions

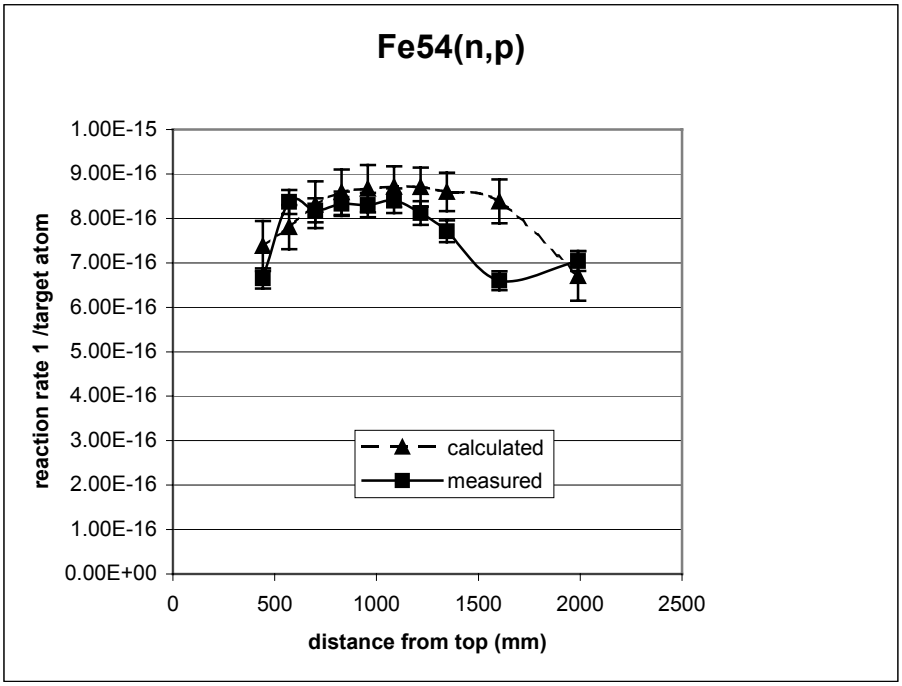

Figure 4. Calculated and measured values of Fe54(n,p) rates in the cavity

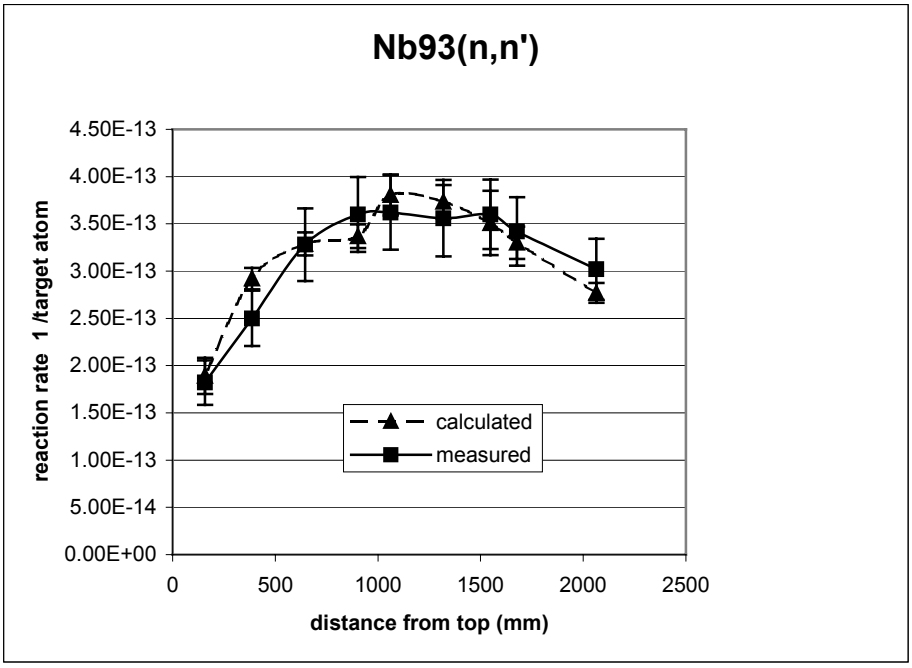

Figure 5. Calculated and measured values of Nb93(n,n') rates at surveillance positions

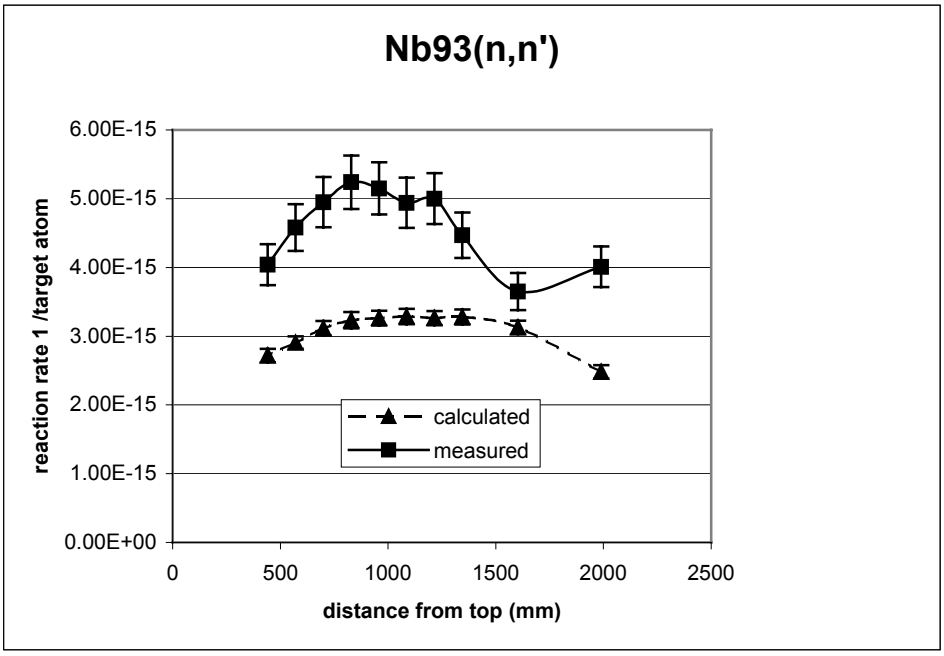

Figure 6. Calculated and measured values of Nb93(n,n') rates in the cavity

The agreement between the measured and calculated values is fairly good at surveillance positions. However, there are discrepancies in the cavity. In the case of Cu63(n,α), the deviation

is not larger, than it would be allowed by the statistical and measurements error, but an apparent tendency of underestimation can be seen. In the case of Fe54(n,p) and Nb93(n,n'), there is a local minimum in the measured data. There is nothing in the computational model, which could produce such a behavior. The most likely explanation is the presence of some mechanical structure in the cavity, which was unknown for the authors at that time of making the model. This assumption will be checked in the near future.

The rate of thermal reactions Nb93(n,γ) and Co59(n,γ) were calculated at the surveillance position close to the midplane. The ratio of the calculated and measured values is shown in Table I.

Table I. The ratio of the calculated and measured thermal reaction rates

	Nb93(n,γ)	Co59(n,γ)
calculated/measured	1.02	0.69

3.2 Uncertainty of the iron cross sections

Beside the local minimum in the cavity (described above), there is a quite good agreement between the measured and calculated reaction rates in the case of Fe54(n,p), but in the case of Nb93(n,n') the differences (at some point as much as 40 %) is significantly higher than that could be explained by statistical and measurement errors. Keeping in mind the good agreement for the same reaction at the surveillance position, this may be due to the error of the iron cross section. The neutrons contributing to the reaction rate in the cavity undergo more collisions than that of contributing to the reaction rate at the surveillance position. This is illustrated on the next figures.

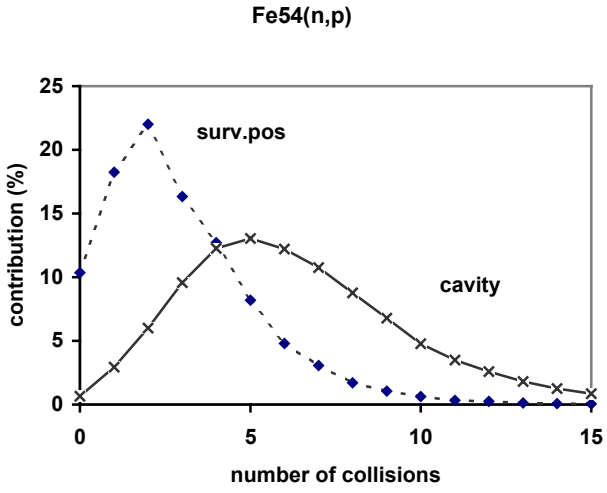

Figure 7 Contribution of the reaction rate Fe54(n,p)

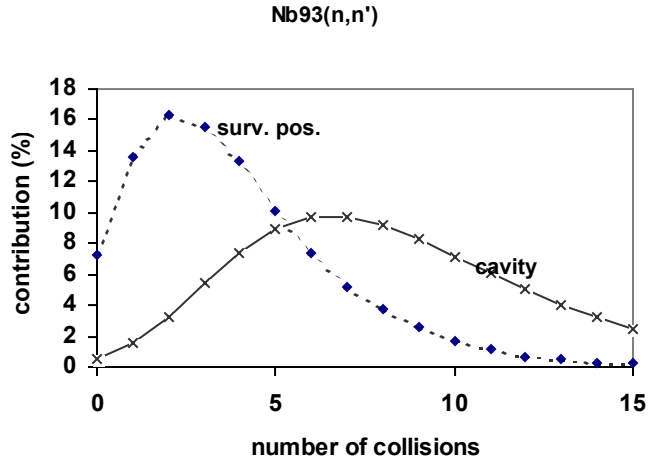

Figure 8. Contribution of the reaction rate Nb93(n,n')

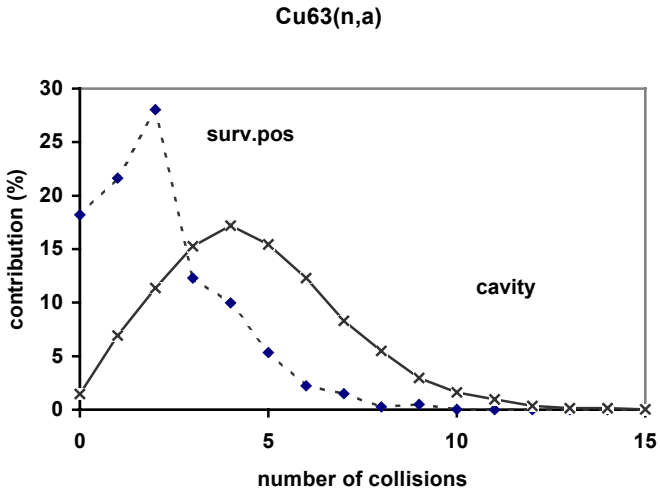

Figure 9. Contribution of the reaction rate Cu63(n,α)

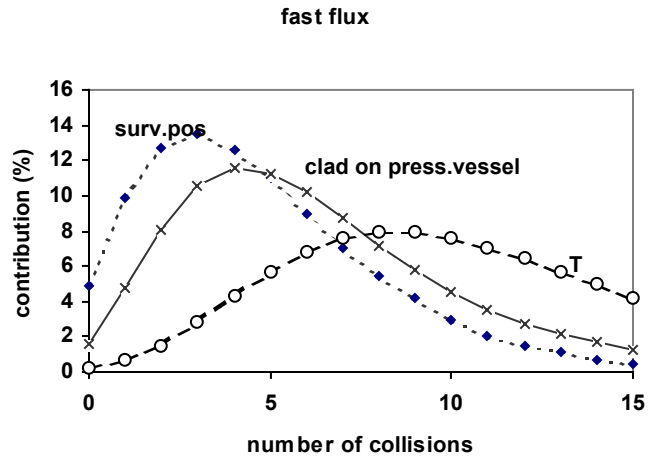

Figure 10. Contribution of the fast flux

The error introduced into the calculations by the uncertainties of the iron cross section was calculated using the covariance data and the sensitivity coefficients. The covariance matrix was calculated by the help of the NJOY code [5]. For determination of the sensitivity coefficients the perturbation capability of the MCNP was used (card PERT). The sensitivity coefficients were determined for the reaction rates Nb93(n,n'), Fe54(n,p) and Cu63(n,α) and the fast flux in the middle axial level but in several different positions of the reactor. The results are summarized in the next tables. "E" means the upper border of the energy group.

Table II. Relative sensitivity of the reaction rates as function of the energy.

E (MeV)	Nb93(n,n')		Fe54(n,p)		Cu63(n,α)	
	surv. pos.	cavity	surv. pos.	cavity	surv. pos.	cavity
10	-1.17E-02	-8.65E-02	-8.26E-02	-3.54E-01	-7.89E-01	-2.06E+00
8.2	-4.37E-02	-2.36E-01	-2.51E-01	-8.04E-01	-6.49E-01	-1.31E+00
6.1	-1.19E-01	-4.32E-01	-4.86E-01	-1.09E+00	-6.06E-02	-9.70E-02
4.1	-1.52E-01	-3.55E-01	-2.87E-01	-4.71E-01	0.00E+00	0.00E+00
3.0	-7.29E-02	-1.84E-01	-7.29E-02	-1.41E-01	0.00E+00	0.00E+00
2.6	-1.36E-01	-3.02E-01	-7.39E-02	-1.40E-01	0.00E+00	0.00E+00
2.1	-7.18E-02	-1.38E-01	-1.30E-02	-2.94E-02	0.00E+00	0.00E+00
1.8	-7.39E-02	-1.39E-01	-7.53E-03	-1.94E-02	0.00E+00	0.00E+00
1.5	-5.76E-02	-1.15E-01	-6.54E-03	-1.61E-02	0.00E+00	0.00E+00
1.2	-3.91E-02	-9.68E-02	-5.86E-03	-1.75E-02	0.00E+00	0.00E+00
0.9	-2.10E-03	-5.49E-03	-4.21E-04	-1.36E-03	0.00E+00	0.00E+00
0.6	0.00E+00	0.00E+00	0.00E+00	0.00E+00	0.00E+00	0.00E+00

One can see from the table that the sensitivity of the reaction rates is more significant in the cavity. It can be interpreted by the more collisions of the neutrons with iron. The energy dependence changes by reaction rates

Table III. Relative sensitivity of the fast flux as function of the energy.

E(MeV)	surv. pos.	Clad	T/4	T/2	T
10	-7.62E-03	-4.59E-02	-5.06E-02	-5.41E-02	-6.19E-02
8.2	-2.65E-02	-1.31E-01	-1.42E-01	-1.54E-01	-1.68E-01
6.1	-6.57E-02	-2.58E-01	-2.77E-01	-2.93E-01	-3.12E-01
4.1	-7.35E-02	-1.96E-01	-2.13E-01	-2.23E-01	-2.34E-01
3.0	-2.94E-02	-9.14E-02	-1.00E-01	-1.06E-01	-1.13E-01
2.6	-6.27E-02	-1.44E-01	-1.63E-01	-1.79E-01	-1.98E-01
2.1	-3.92E-02	-6.35E-02	-7.39E-02	-8.44E-02	-9.81E-02
1.8	-3.91E-02	-5.39E-02	-5.65E-02	-6.29E-02	-7.94E-02
1.5	-5.99E-02	-5.21E-02	-7.03E-02	-8.45E-02	-1.06E-01
1.2	-6.48E-02	-4.90E-02	-7.91E-02	-1.03E-01	-1.40E-01
0.9	-5.13E-03	-3.80E-03	-7.10E-03	-9.49E-03	-1.25E-02

The sensitivity increases with the distance from the core. The energy dependence changes from place to place due to the change of the spectrum.

Summarizing the results the total errors of the calculated values due to the uncertainty of the iron cross section can be seen in the next tables.

Table IV. Uncertainty of the calculated fast flux due to the iron cross section error

position	Δ (%)
surveillance pos.	4.0
clad of the vessel	6.6
T/4	7.6
T/2	8.5
T	10.9

Table V. Uncertainty of the calculated reaction rates due to the the iron cross section error

	SURV. POS. Δ (%)	CAVITY Δ (%)
Fe54 (n,p)	8	20
Nb93 (n,n')	6	14
Cu63 (n,α)	9	22

As it is supposed, the error is essentially higher in the cavity than at the surveillance positions. In the case of the Nb93(n,n') the error is 14 % in the cavity. This value is still a little low to explain the difference of measured and calculated values in the cavity. This suggests that this deviation may be due to the reaction cross section error or some inaccuracy in the model.

4. SUMMARY

Reaction rates were calculated and measured for different axial positions in surveillance position and in the cavity of Unit II. of the Paks NPP. Detailed operational history of the reactor was taken into account in deriving the neutron source. A surface source was used instead of volume source to accelerate the Monte Carlo calculations. A fairly good agreement was found in most of the cases. However, the deviation found in some cases suggests further investigation of the used cross sections and modeling details.

REFERENCES

1. Gadó, J., Hegedűs, Cs., Hegyi Gy., Keresztúri, A., Makai, M., Maráczy, Cs., Telbisz, M, KARATE – A Code for VVER-440 Core Calculation, In: *Proc. of the ANS Winter Meeting, Washington, DC,* **Vol. 71**, pp. 485-487.

2. Gadó, J., Keresztúri, A., Trosztel, I., 1990. The Program System KARATE. In: *Proc. of IAEA Specialists Mtg. Advanced Calculational Methods for Power Reactors*, Cadarache, France
3. E. Temesvári,Gy. Hegyi, A. Keresztúri, Cs. Maráczy, Neutron Fluence Calculations for The Reactor Vessel, In: *Proc. of the Mathematics and Computation,* Salt Lake City, Utah, USA, September 2001
4. J. Breismeister (Editor); MCNP™ - A General Monte Carlo N-Particle Transport Code - Version 4C, LA-13709-M, 2000
5. R.E.MacFarlane, D.W.Muir, The NJOY Nuclear Data Processing System, Version 91, LA-12740-M, 1994